

Irradiation and Flame Retardant Effect of Poly[bis(phenoxyphosphazene)] and Magnesium Hydroxide in LDPE Composites (Postprint)

Authors: LI Jian-Xi, Zhang Cong, Chen Tao, LI Lin-Fan, LI Jing-Ye

Date: 2023-06-18T00:00:00+00:00

Abstract

Poly[bis(phenoxyphosphazene)] (PBPP) and magnesium hydroxide (MH) are used as a flame retardant blend with low-density polyethylene (LDPE) for the nuclear cable. This study aims to investigate the effects of PBPP in MH-LDPE blend composites on flame retardance and electron beam irradiation. The structure, morphology, and properties of the blend composites irradiated by an electron beam to different absorbed doses were characterized. The results indicated that PBPP provides lubrication during processing. As the PBPP content in the blend increases the melt flow rate at 20 phr MH, meaning the material is easier to process. The higher the PBPP content, the higher the limiting-oxygen index. The elongation at the break of the PBPP containing composites (at 50 phr MH) was evidently higher than the non-PBPP ones at different absorbed doses by electron beam irradiation. The thermogravimetric analysis results indicated that the improved mechanical property, resulting from electron-beam irradiation, could be attributed to the consumption of PBPP.

Full Text

Preamble

Adsorption Behaviors of Iodide Anion on Silver Loaded Macroporous Silicas

WU Hao, WU Yan,[†] CHEN Zi, and WEI Yue-Zhou

School of Nuclear Science and Engineering, Shanghai Jiao Tong University, Shanghai 200240, China

(Received July 31, 2014; accepted in revised form October 13, 2014; published online June 20, 2015)

A macroporous silica-based silver loaded adsorbent was synthesized by grafting the silver complexes of thiourea ($\text{Ag}(\text{tu})_3\text{NO}_3$) into a silica-based copolymer

support ($\text{SiO}_2\text{-P}$). The adsorbent was used to uptake iodide anions (I^-) via batch and column techniques. Kinetic and saturated adsorption experiments were carried out by varying shaking times and initial I^- concentrations. Experimental results showed that kinetic adsorption of I^- was controlled by a pseudo second-order model, while saturated adsorption was governed by a chemisorption mechanism following a Langmuir adsorption equation. The breakthrough curve of I^- exhibited an S-shaped profile, with column efficiency estimated to exceed 90%.

Keywords: Iodide anion, Silver complexes of thiourea, Grafting, Macroporous silica-based support, Radioactive contaminated wastewater

DOI: 10.13538/j.1001-8042/nst.26.030301

Introduction

Large quantities of radioactive contaminated wastewater (RCW) were generated during the Fukushima NPP-1 nuclear accident in Japan. The RCW consists of reactor cooling water that contacted damaged nuclear fuel debris, with primary radionuclides including soluble cesium (^{134}Cs , ^{137}Cs), strontium (^{90}Sr), and iodine (^{131}I , ^{129}I) [1]. With a half-life of 1.7×10^7 years, ^{129}I represents a primary long-term risk driver in shallow land disposal facilities, while ^{131}I poses acute contamination risks due to its short half-life of 8.05 days and high specific activity [2]. Untreated iodine contaminants released into the environment would pollute soil, air, and groundwater, creating long-term radioecological hazards.

Aqueous iodine exists primarily as iodide (I^-) and iodate (IO_3^-) anions, depending on redox conditions and pH. At low to neutral pH with positive redox potentials, the iodide anion dominates in solution [3]. The Fukushima RCW contains various coexisting components from seawater (saline elements), corrosion products, and groundwater, with pH ranging from 7-8 [4]. Previous studies have developed various methods to remove or adsorb iodide anions from aqueous solutions [5-7]. Common natural porous materials such as alumina and hydrotalcite can adsorb iodide anions through surface physical adsorption or ion exchange with active groups [8]. However, coexisting chloride anions in RCW compete with iodide anions, rendering these natural materials non-selective for iodide. Inorganic anion exchangers such as $\text{BiPbO}_2(\text{NO}_3)$ have also been reported to adsorb iodide anions [9], but these materials are often difficult to prepare and may pose toxicity concerns. Cuprous (Cu^+)-containing compounds react with iodide anions to form cuprous iodide through hydrogen anion participation, but this process is highly pH-sensitive, resulting in low adsorption capacity in neutral and slightly acidic solutions [10]. Silver-based adsorbents have been investigated more recently; their adsorption mechanism relies on strong chemical interaction between silver and iodide anions, offering good selectivity. However, leaching of impregnated materials can reduce adsorption capacity [11].

In this work, we synthesized a macroporous silica-based silver loaded adsorbent ($\text{Ag}(\text{tu})_3\text{NO}_3/\text{SiO}_2\text{-P}$) by grafting silver complexes of thiourea ($\text{Ag}(\text{tu})_3\text{NO}_3$)

into a silica-based copolymer support ($\text{SiO}_2\text{-P}$) for iodide anion adsorption. The $\text{SiO}_2\text{-P}$ support is an inorganic macroporous material prepared by impregnating copolymer inside macroporous SiO_2 substrate [12]. Grafting $\text{Ag}(\text{tu})_3\text{NO}_3$ into $\text{SiO}_2\text{-P}$ offers several advantages, including mechanical strength, strong acid and chemical stability, radiation resistance, and ease of solid-liquid separation. Compared to reported iodide adsorbents, the synthesized $\text{Ag}(\text{tu})_3\text{NO}_3/\text{SiO}_2\text{-P}$ is easy to prepare and prevents silver leaching during adsorption. This study investigates the adsorption kinetics, mechanisms, and dynamic adsorption behavior of iodide anions on $\text{Ag}(\text{tu})_3\text{NO}_3/\text{SiO}_2\text{-P}$.

Experimental

A. Materials

Reagents used in the experiments—including sulfuric acid (98%), nitric acid (65%), hydrochloric acid (37%), ethanol, tin(II) chloride dihydrate, ammonium thiocyanate, and silver nitrate—were analytical grade or better. The $\text{SiO}_2\text{-P}$ support was synthesized using a known method [13]; for simplicity, “P” in $\text{SiO}_2\text{-P}$ denotes the styrene-divinylbenzene (SDB) copolymer immobilized inside the macroporous SiO_2 substrate through polymerization.

B. Preparation of $\text{Ag}(\text{tu})_3\text{NO}_3/\text{SiO}_2\text{-P}$

The synthesis of $\text{Ag}(\text{tu})_3\text{NO}_3/\text{SiO}_2\text{-P}$ proceeded through four steps (Fig. 1 [Figure 1: see original paper]): (1) $\text{SiO}_2\text{-P-NO}_2$ was prepared by nitrating the copolymer in $\text{SiO}_2\text{-P}$ through mixing with nitric acid (65%) and sulfuric acid (98%) in a water bath at 50 °C for 3 h. (2) $\text{SiO}_2\text{-P-NO}_2$ was reduced to $\text{SiO}_2\text{-P-NH}_2$ using stannous chloride, hydrochloric acid (37%), and ethanol in a water bath at 60 °C for 12 h. (3) $\text{SiO}_2\text{-P-tu}$ was prepared by mixing $\text{SiO}_2\text{-P-NH}_2$, ethanol, and ammonium thiocyanate in a flask with water bath heating at 70 °C, stirring for 12 h, followed by filtration and drying at 50 °C. (4) $\text{Ag}(\text{tu})_3\text{NO}_3/\text{SiO}_2\text{-P}$ was prepared by mixing $\text{SiO}_2\text{-P-tu}$ with silver nitrate solution in a flask, stirring for 12 h, then filtering and drying at 50 °C. Numerous structural types of $\text{Ag}(\text{I})/(\text{x})\text{tu}$ ($\text{x}=1\text{--}n$) complexes have been reported, with $\text{Ag}(\text{I})/(3)\text{tu}$ complexes being the most common [14–17].

C. Characterization

SEM analysis (Nova NanoSEM NPE218) examined the surface morphology of $\text{Ag}(\text{tu})_3\text{NO}_3/\text{SiO}_2\text{-P}$. Thermal stability of $\text{SiO}_2\text{-P}$ and $\text{Ag}(\text{tu})_3\text{NO}_3/\text{SiO}_2\text{-P}$ was evaluated using TG-DTA equipment (Shimadzu DTG-60) at a constant heating rate of 10 °C/min from 25 °C to 800 °C. The FT-IR spectrum of $\text{Ag}(\text{tu})_3\text{NO}_3/\text{SiO}_2\text{-P}$ was recorded from 4000–500 cm^{-1} using an IRAffinity-1 FT-IR spectrometer.

D. Static Experiments

Static adsorption behavior of iodide anions on the adsorbent was examined through batch experiments using $\text{Ag}(\text{tu})_3\text{NO}_3/\text{SiO}_2\text{-P}$. An aqueous phase (5 mL) containing varying iodide anion concentrations was equilibrated with 0.1 g adsorbent in stoppered glass tubes in a thermostatic water bath (Tokyo RIKAKIKA Co., Ltd.) at room temperature. Iodide anion concentrations before and after adsorption were measured by ICP-AES (Shimadzu 7510). The equilibrium adsorption capacity (Q_{eq}) was calculated using:

$$Q_{eq} = \frac{V}{m} \times (C_0 - C_e)$$

where C_0 and C_e are the initial and equilibrium concentrations of iodide anions, m is the adsorbent weight, and V is the aqueous phase volume.

E. Column Operation

$\text{Ag}(\text{tu})_3\text{NO}_3/\text{SiO}_2\text{-P}$ (4.05 g) was densely packed into a glass column (10 mm diameter, 200 mm length) with a thermo jacket set at $(25 \pm 1)^\circ\text{C}$ (Fig. 2 [Figure 2: see original paper]). Iodide anion breakthrough was tested using a feed solution of 1 mM NaI at a flow rate of $0.5\text{ cm}^3/\text{min}$.

Results and Discussion

A. SEM

SEM micrographs of $\text{Ag}(\text{tu})_3\text{NO}_3/\text{SiO}_2\text{-P}$ (Fig. 3 [Figure 3: see original paper]) revealed obvious spherical and porous particles with an estimated practical size of $50\text{ }\mu\text{m}$ in diameter. The smooth surface indicated that active ingredients were impregnated inside the $\text{SiO}_2\text{-P}$ matrix.

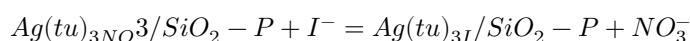
B. TG-DTA

TG-DTA results for $\text{SiO}_2\text{-P}$ (Fig. 4 [Figure 4: see original paper]) showed two weight loss ranges: $280\text{--}350^\circ\text{C}$ and $350\text{--}550^\circ\text{C}$, both attributed to thermal desorption of the SDB copolymer [18]. The overall weight loss of $\text{SiO}_2\text{-P}$ was approximately 15%, indicating 15 wt.% SDB impregnation and 85 wt.% SiO_2 content.

TG-DTA results for $\text{Ag}(\text{tu})_3\text{NO}_3/\text{SiO}_2\text{-P}$ (Fig. 5 [Figure 5: see original paper]) showed three weight loss ranges. The first and second losses corresponded to SDB polymer burning, similar to Fig. 4. The third weight loss ($400\text{--}550^\circ\text{C}$) represented thermal decomposition of the silver-thiourea complex, with a corresponding endothermic peak around 540°C . The silver-thiourea complex content grafted onto the copolymer was estimated to be 12%.

C. Kinetic Adsorption Studies

The effect of contact time on iodide anion adsorption by $\text{Ag}(\text{tu})_3\text{NO}_3/\text{SiO}_2\text{-P}$ was investigated. The relationship between adsorption time (t) and amount adsorbed at time t (q_t) is plotted in Fig. 6 [Figure 6: see original paper]. Adsorption equilibrium for iodide anions (I^-) on $\text{Ag}(\text{tu})_3\text{NO}_3/\text{SiO}_2\text{-P}$ was attained within 10 min in pure water, with an adsorbed amount of 8.89 mg/g. In 0.6 M NaCl solution (simulated seawater), equilibrium time was similar to that in pure water. The uptake of I^- by $\text{Ag}(\text{tu})_3\text{NO}_3/\text{SiO}_2\text{-P}$ was governed by the ion-exchange reaction:



The thiourea (tu) functional group's ability to form stable adducts with silver is well established [16]. $\text{Ag}(\text{tu})^+$ differs from Ag^+ in that $\text{Ag}(\text{tu})_3^+$ does not react with Cl^- [24, 25], making $\text{Ag}(\text{tu})_3\text{NO}_3/\text{SiO}_2\text{-P}$ effective for I^- removal from seawater.

To investigate the adsorption mechanism and determine the rate-controlling step, experimental data were tested using the pseudo second-order kinetic model:

$$\frac{dq_t}{dt} = K_2 \times (Q_{eq} - q_t)^2$$

Integrating Eq. (3) with boundary conditions (1) at $t = 0$ and $q_t = 0$ and (2) at $t = t$ and $q_t = q_t$ yields:

$$\frac{t}{q_t} = \frac{1}{K_2 Q_{eq}^2} + \frac{t}{Q_{eq}}$$

where K_2 (mg/(g · min)) is the adsorption rate constant for pseudo second-order kinetics, q_t (mg/g) is the amount of iodide anions adsorbed at time t , and Q_{eq} (mg/g) is the amount adsorbed at equilibrium [26]. The fit lines (Fig. 8 [Figure 8: see original paper]) show regression values greater than 0.99, indicating the adsorption system follows second-order kinetics. Q_{eq} and K_2 can be determined from a plot of t/q_t versus t , with calculated values summarized in Table 1. The calculated Q_{eq} values agree with experimental data, indicating I^- adsorption was a rate-controlled step governed by chemisorption.

D. FT-IR Studies

The FT-IR spectrum of $\text{Ag}(\text{tu})_3\text{NO}_3/\text{SiO}_2\text{-P}$ is shown in Fig. 7 [Figure 7: see original paper]. Since $\text{Ag}(\text{tu})_3\text{NO}_3$ was grafted into $\text{SiO}_2\text{-P}$ pores, the spectrum (Fig. 7(a)) was dominated by Si-O groups. Enlarged details are shown in Figs. 7(b)-7(d). The sharp band at 1080 cm^{-1} (Fig. 7(a)) corresponds to asymmetric

Si–O–Si vibrations, while the band at 789 cm^{-1} represents symmetric Si–O stretching [19]. After nitration, $\text{SiO}_2\text{-P}$ showed peaks at 1518 cm^{-1} and 1350 cm^{-1} , corresponding to N–O asymmetric and symmetric stretches. Asymmetric and symmetric vibrations of NH_2 groups appeared between 3231 cm^{-1} and 3178 cm^{-1} (Figs. 7(d)) [20]. The small shoulder at 1560 cm^{-1} in Fig. 7(c) was due to (C–S), indicating C–S group coordination to the Ag atom in the complex. The band at 768 cm^{-1} was assigned to C–S group bending vibration, further supporting C–S coordination to Ag [21, 22].

E. Adsorption Isotherms

Langmuir and Freundlich isotherm models were studied to elucidate the adsorption mechanism of iodide anions (I^-) on $\text{Ag}(\text{tu})_3\text{NO}_3/\text{SiO}_2\text{-P}$. Isotherm parameters were determined using Origin software, which plotted C_{eq} versus Q_{eq} for different isotherms.

1. Langmuir Isotherm The Langmuir isotherm is given by:

$$\frac{C_{eq}}{Q_{eq}} = \frac{1}{K_L Q_{max}} + \frac{C_{eq}}{Q_{max}}$$

where Q_{max} is the maximum monolayer adsorption capacity (mg/g), K_L is the equilibrium constant related to free energy (L/mg), C_{eq} is the equilibrium iodide anion concentration (mg/L), and Q_{eq} is the amount adsorbed at equilibrium (mg/g) [27].

2. Freundlich Isotherm The Freundlich isotherm applies to multilayer adsorption on heterogeneous surfaces:

$$\lg Q_{eq} = \frac{1}{n} \lg C_{eq} + \lg K_F$$

where Q_{eq} is the amount adsorbed at equilibrium (mg/g), C_{eq} is the equilibrium concentration (mg/L), n measures deviation from adsorption linearity, and K_F is the multilayer adsorption capacity (mg/g).

The linear plot of C_{eq}/Q_{eq} versus C_{eq} shows adsorption follows a Langmuir isotherm (Fig. 9 [Figure 9: see original paper]), suggesting monolayer coverage of iodide anions on $\text{Ag}(\text{tu})_3\text{NO}_3/\text{SiO}_2\text{-P}$ surfaces. Q_{max} and K_L values were calculated from slope and intercept (Table 2). The Q_{max} value for $\text{Ag}(\text{tu})_3\text{NO}_3/\text{SiO}_2\text{-P}$ in 0.6 M NaCl was 8.96 mg/g, similar to that in pure water. In contrast, Freundlich plots showed low R^2 values around 0.6 (Fig. 10 [Figure 10: see original paper]), indicating poor applicability of the Freundlich isotherm.

F. Column Experiments

Fixed-bed adsorption performance was evaluated through dynamic column studies, expressed as breakthrough curves relating outlet concentration (C) to inlet concentration (C_0) versus effluent volume for a given bed height [16]. Iodide breakthrough was tested using 1 mM NaI feed solution at 0.5 cm³/min flow rate. The breakthrough curve (Fig. 11 [Figure 11: see original paper]) shows an S-shaped profile with steep slope, indicating no Ag(tu)₃NO₃ dislodgement from the SiO₂-P matrix. The 5% breakthrough point occurred at 235 cm³ (pure water) and 231 cm³ (0.6 M NaCl), with complete exhaustion at approximately 284 cm³ and 286 cm³, respectively. Breakthrough capacity (B.T. Cap.) and total capacity (T. Cap.) were calculated as 7.24 mg/g and 7.87 mg/g in 0.6 M NaCl solution, yielding high column efficiency (B.T. Cap./T. Cap.) of 91.9%. Adsorption behavior in pure water closely matched that in 0.6 M NaCl, demonstrating that Cl⁻ anions did not affect I⁻ adsorption. The Ag(tu)₃NO₃/SiO₂-P packed column effectively removed I⁻ from radioactive contaminated wastewater, even with high NaCl concentrations.

Conclusion

A macroporous silica-based Ag(tu)₃NO₃/SiO₂-P resin was prepared by grafting Ag(tu)₃NO₃ onto SiO₂ support. Iodide uptake properties were investigated via batch methods, with adsorption behaviors further studied by column methods in pure water and 0.6 M NaCl solution. Thermal stability analysis indicated that Ag(tu)₃NO₃/SiO₂-P maintains adsorption capability up to 200 °C. Iodide adsorption was rapid in both pure water and 0.6 M NaCl solution, reaching equilibrium within 10 min. Kinetic data were successfully modeled using the pseudo second-order kinetic model. Iodide adsorption fit the Langmuir model well, with correlation coefficients (R^2) exceeding 0.99, suggesting monolayer adsorbent coverage on Ag(tu)₃NO₃/SiO₂-P surfaces. The adsorbent effectively removed iodide anions in 0.6 M NaCl column operations. These results demonstrate that Ag(tu)₃NO₃/SiO₂-P is an efficient adsorbent for separating iodide anions from radioactive wastewater.

References

- [1] Sylvester P, Milner T and Jensen J. Radioactive liquid waste treatment at Fukushima Daiichi. *J Chem Technol Biot*, 2013, 88: 1592-1596. DOI: 10.1002/jctb.4141
- [2] Hu Q H, Zhao P H, Moran J E, et al. Sorption and transport of iodine species in sediments from the Savannah River and Hanford Sites. *J Contam Hydrol*, 2005, 78: 185-205. DOI: 10.1016/j.jconhyd.2005.05.007
- [3] Karanfil T, Moro E C and Serkiz S M. Development and testing of a silver chloride-impregnated activated carbon for aqueous removal and sequestration of iodide. *Environ Technol*, 2005, 26: 1255-1262. DOI: 10.1080/09593332608618595

- [4] Sachse A, Merceille A, Barré Y, et al. Macroporous LTA-monoliths for in-flow removal of radioactive strontium from aqueous effluents: Application to the case of Fukushima. *Microporous Mesoporous Mater*, 2012, 164: 251-258. DOI: 10.1016/j.micromeso.2012.07.019
- [5] Nagata T, Fukushi K and Takahashi Y. Prediction of iodide adsorption on oxides by surface complexation modeling with spectroscopic confirmation. *J Colloid Interf Sci*, 2009, 332: 309-316. DOI: 10.1016/j.jcis.2008.12.037
- [6] Brown C F, Geiszler K N and Vickerman T S. Extraction and quantitative analysis of iodine in solid and solution matrixes. *Anal Chem*, 2005, 77: 7062-7066. DOI: 10.1021/ac050972v
- [7] Ensafi A A and Eskandari H. Efficient and selective extraction of iodide through a liquid membrane. *Microchem J*, 2001, 69: 45-50. DOI: 10.1016/S0026-265X(00)00188-0
- [8] Dai J L, Zhang M, Hu Q H, et al. Adsorption and desorption of iodine by various Chinese soils: iodide and iodate. *Geoderma*, 2009, 153: 130-135. DOI: 10.1016/j.geoderma.2009.07.020
- [9] Kodama H and Kabay N. Reactivity of inorganic anion exchanger BiPbO₂(NO₃) with fluoride ions in solution. *Solid State Ionics*, 2001, 141-142: 603-607. DOI: 10.1016/S0167-2738(01)00775-5
- [10] Lefèvre G, Walcarius A, Ehrhardt J J, et al. Sorption of iodide on cuprite (Cu₂O). *Langmuir*, 2000, 16: 4519-4527. DOI: 10.1021/la9903999
- [11] Zhang H F, Gao X L, Guo T, et al. Adsorption of iodide ions on a calcium alginate-silver chloride composite adsorbent. *Colloid Surface A*, 2011, 386: 166-171. DOI: 10.1016/j.colsurfa.2011.07.014
- [12] Wu Y, Kim S Y, Tozawa D, et al. Study on selective separation of cesium from high level liquid waste using a macroporous silica-based supramolecular recognition adsorbent. *J Radioanal Nucl Ch*, 2012, 293: 13-20. DOI: 10.1007/s10967-012-1738-6
- [13] Wei Y Z, Kumagai M, Takashima Y, et al. Studies on the separation of minor actinides from high-level wastes by extraction chromatography using novel silica-based extraction resins. *Nucl Technol*, 2000, 132: 413-423.
- [14] Bowmaker G A, Skelton B W and White A H. Structural and infrared spectroscopic studies of some novel mechanochemically accessed adducts of silver(I) oxoanion salts with thiourea. *Inorg Chem*, 2009, 48: 3185-3197. DOI: 10.1021/ic802312j
- [15] Pleysier J and Cremers A. Stability of silver-thiourea complexes in montmorillonite clay. *J Chem Soc*, 1975, 71: 256-264. DOI: 10.1039/F19757100256
- [16] Ahmad S, Isab A A and Perzanowski H P. Silver(I) complexes of thiourea. *Transit Metal Chem*, 2002, 27: 782-785. DOI: 10.1023/A:1020350023536
- [17] Murthy D S R and Prasad P M. Leaching of gold and silver from Miller Process dross through non-cyanide leachants. *Hydrometallurgy*, 1996, 42: 27-33. DOI: 10.1016/0304-386X(95)00049-M
- [18] Wu Y, Kim S Y, Tozawa D, et al. Equilibrium and kinetic studies of selective adsorption and separation for strontium using DtBuCH18C6 loaded resin. *J Nucl Sci Technol*, 2012, 49: 320-327. DOI: 10.1080/00223131.2012.660022
- [19] Mülle K, Foerstendorf H, Brendler V, et al. Sorption of Np(V) onto TiO₂,

- SiO₂, and ZnO: An in situ ATR FT-IR spectroscopic study. Environ Sci Technol, 2009, 43: 7665-7670. DOI: 10.1021/es901256v
- [20] Lala N L, Deivaraj T C and Lee J Y. Auto-deposition of gold on chemically modified polystyrene beads. Colloid Surface A, 2005, 269: 119-124. DOI: 10.1016/j.colsurfa.2005.06.073
- [21] Joseph G P, Rajarajan K, Vimalan M, et al. Spectroscopic, thermal and mechanical behavior of allylthiourea cadmium chloride single crystals. Mater Res Bull, 2007, 42: 2040-2047. DOI: 10.1016/j.materresbull.2007.02.002
- [22] Bowmaker G A, Skelton B W and White A H. Structural and infrared spectroscopic studies of some novel mechanochemically accessed adducts of silver(I) oxoanion salts with thiourea. Inorg Chem, 2009, 48: 3185-3197. DOI: 10.1021/ic802312j
- [23] El Aamrani F Z, Sastre A, Aguilar M, et al. Iodide-selective electrodes based on the silver(I) complex of a novel N-thiocarbamoylimine-dithioether derivative. Anal Chim Acta, 1996, 329: 247-252. DOI: 10.1016/0003-2670(96)00115-8
- [24] Sandberg R G and Huiatt J L. Ferric chloride, thiourea and brine leach recovery of Ag, Au and Pb from complex sulfides. JOM, 1986, 38: 18-22. DOI: 10.1007/BF03257810
- [25] El Aamrani F Z, Garcia-Raurich J, Sastre A, et al. PVC membranes based on silver(I)-thiourea complexes. Anal Chim Acta, 1999, 402: 129-135. DOI: 10.1016/S0003-2670(99)00562-0
- [26] Senthilkumar T, Raghuraman R and Miranda L R. Parameter optimization of activated carbon production from Agave sisalana and Punica granatum peel: adsorbents for C.I. reactive orange 4 removal from aqueous solution. Clean, 2013, 41: 797-807. DOI: 10.1002/clen.201100719
- [27] Jain R, Sharma P and Sikarwar S. Kinetics and isotherm analysis of Tropaeoline 000 adsorption onto unsaturated polyester resin (UPR): a non-carbon adsorbent. Environ Sci Pollut R, 2013, 20: 1493-1502. DOI: 10.1007/s11356-012-0994-x

Note: Figure translations are in progress. See original paper for figures.

Source: ChinaXiv – Machine translation. Verify with original.